follow-up angiography at 10 months after PCI was performed in all patients, and percent diameter stenosis was significantly smaller in the group with calcium fracture compared with the group without calcium fracture (19 ± 27% vs. 38 ± 38%; p = 0.030). The frequency of binary restenosis (14% vs. 41%; p = 0.024) and ischemic-driven target lesion revascularization (7% vs. 28%; p = 0.046) were significantly lower in the group with calcium fracture compared with the group without calcium fracture.

OCT offers a unique opportunity to observe plaque modification after PCI in the severe calcified lesion. Coronary calcium fracture by PCI was associated with adequate stent expansion and favorable late outcomes. Our findings support and underline the need for optimal lesion preparation in the treatment of heavily calcified lesions.

Takashi Kubo, MD, PhD*
Kunihiro Shimamura, MD
Yasushi Ino, MD, PhD
Tomoyuki Yamaguchi, MD
Yoshiki Matsuo, MD, PhD
Yasutsugu Shiono, MD
Akira Taruya, MD
Tsuyoshi Nishiguchi, MD
Aiko Shimokado, MD
Ikuko Teraguchi, MD, PhD
Makoto Orii, MD
Takashi Yamano, MD
Takashi Tanimoto, MD, PhD
Hironori Kitabata, MD, PhD
Kumiko Hirata, MD, PhD
Atsushi Tanaka, MD, PhD
Takashi Akasaka, MD, PhD

*Department of Cardiovascular Medicine
Wakayama Medical University
811-1 Kimiidera
Wakayama, 641-8509
Japan
E-mail: takakubo@wakayama-med.ac.jp

http://dx.doi.org/10.1016/j.jcmg.2014.11.012

Please note: Drs. Kubo and Akasaka have received lecture fees from St. Jude Medical and Terumo. All other authors have reported that they have no relationships relevant to the contents of this paper to disclose.

REFERENCES

1. Madhavan MV, Tarigopula M, Mintz GS, et al. Coronary artery calcification: pathogenesis and prognostic implications. J Am Coll Cardiol 2014;63:1703–14.

2. Kobayashi Y, Okura H, Kume T, et al. Impact of target lesion coronary calcification on stent expansion. Circ J 2014;78:2209–14.

3. Vaquerizo B, Serra A, Miranda F, et al. Aggressive plaque modification with rotational atherectomy and/or cutting balloon before drug-eluting stent implantation for the treatment of calcified coronary lesions. J Interv Cardiol 2010;23:240–8.

4. Mintz GS, Popma JJ, Pichard AD, et al. Patterns of calcification in coronary artery disease: a statistical analysis of intravascular ultrasound and coronary angiography in 1155 lesions. Circulation 1995;91:1959–65.

Myocardial Kinetics of a Novel [^{18}F]-Labeled Sympathetic Nerve PET Tracer LMI1195 in the Isolated Perfused Rabbit Heart

A radionuclide tracer approach is a unique assay to monitor the cardiac sympathetic nervous system in patients, and the most widely available tracer is the radiolabeled norepinephrine analogue [^{123}I]-metaiodobenzylguanidine ([^{123}I]-MIBG). A novel ^{18}F-labeled positron emission tomography (PET) tracer, [^{18}F]-LMI1195 (N-[3-bromo-4-(3-[^{18}F]fluoropropoxy)-benzyl]-guanidine), has been developed to overcome the limitations of conventional tracers (1). [^{18}F]-LMI1195 shares similarities with [^{123}I]-MIBG based on its benzylguanidine structure, but higher sensitivity and specificity and more accurate quantification are expected via the general advantages of PET over single-photon emission computed tomography technology. The high specificity of [^{18}F]-LMI1195 for the norepinephrine transporter was confirmed with a cell-binding assay and in vivo imaging (1,2). Most recently, a human volunteer study demonstrated promising results with uniform tracer uptake in the ventricular wall and acceptable radiation doses (3).

We aimed to evaluate further tracer kinetics at the nerve terminal. First-pass tracer extraction fraction (EF) and washout were measured in isolated rabbit hearts (New Zealand White) to avoid systemic recirculation and metabolism of the tracer.

The EF was determined at different flow values (n = 19). Additionally, the influence of desipramine hydrochloride (40 nM) added into the buffer (n = 5) and reserpine-pre-treated hearts (n = 5) were tested. Reserpine pre-treatment was performed with intravenous injection of reserpine (2 mg/kg) 3 h before the study.

A second protocol was designed to measure tracer washout. Hearts were perfused with [^{18}F]-LMI1195 added to the buffer for 10 min (incubation phase) followed by 25 min of perfusion without tracer (washout phase). The tracer washout was examined by control Krebs-Henseleit bicarbonate buffer (n = 9), and desipramine was added (desipramine-chase; n = 5), with washout with electrical field stimulation (5 Hz, 5 V, 1 min × 5 times at the washout phase; n = 7).

JACC: CARDIOVASCULAR IMAGING, VOL. 8, NO. 10, 2015
OCTOBER 2015:1228–34

There was a flow-dependent decrease in the EF, with 44.4 ± 5.1%, 28.1 ± 6.5%, and 21.5 ± 5.1% using flow values of 2, 4, and 8 ml/min/g, respectively. Desipramine, a specific neural uptake-1 blocker, decreased the EF significantly from 28.1 ± 6.5% (control) to 4.3 ± 3.8% ($p < 0.001$). Reserpine, an irreversible vesicular monoamine transporter blocker, pre-treatment did not change the EF (30.1 ± 3.4%; p = NS) (Figure 1).

There was tracer washout with 0.73 ± 0.18 %/min in the first 20-min measurement. Desipramine added only during washout phase did not change the washout rate (0.94 ± 0.12 %/min). On the other hand, electrical field stimulation to enhance the vesicular release of norepinephrine increased the washout rate significantly (1.96 ± 0.48 %/min; $p < 0.01$).

In summary, we measured the myocardial kinetics of [^{18}F]-LMI1195 with isolated perfused rabbit hearts. Specific uptake at the nerve terminal was confirmed by desipramine sensitive uptake. Furthermore, we observed enhanced tracer washout with electrical stimulation, as well as resistance for desipramine chase, suggesting that the tracer handling in the nerve terminals was consistent with norepinephrine vesicular storage and release.

FIGURE 1 Myocardial Kinetics of Novel [^{18}F]-LMI1195 Sympathetic Nervous Tracer

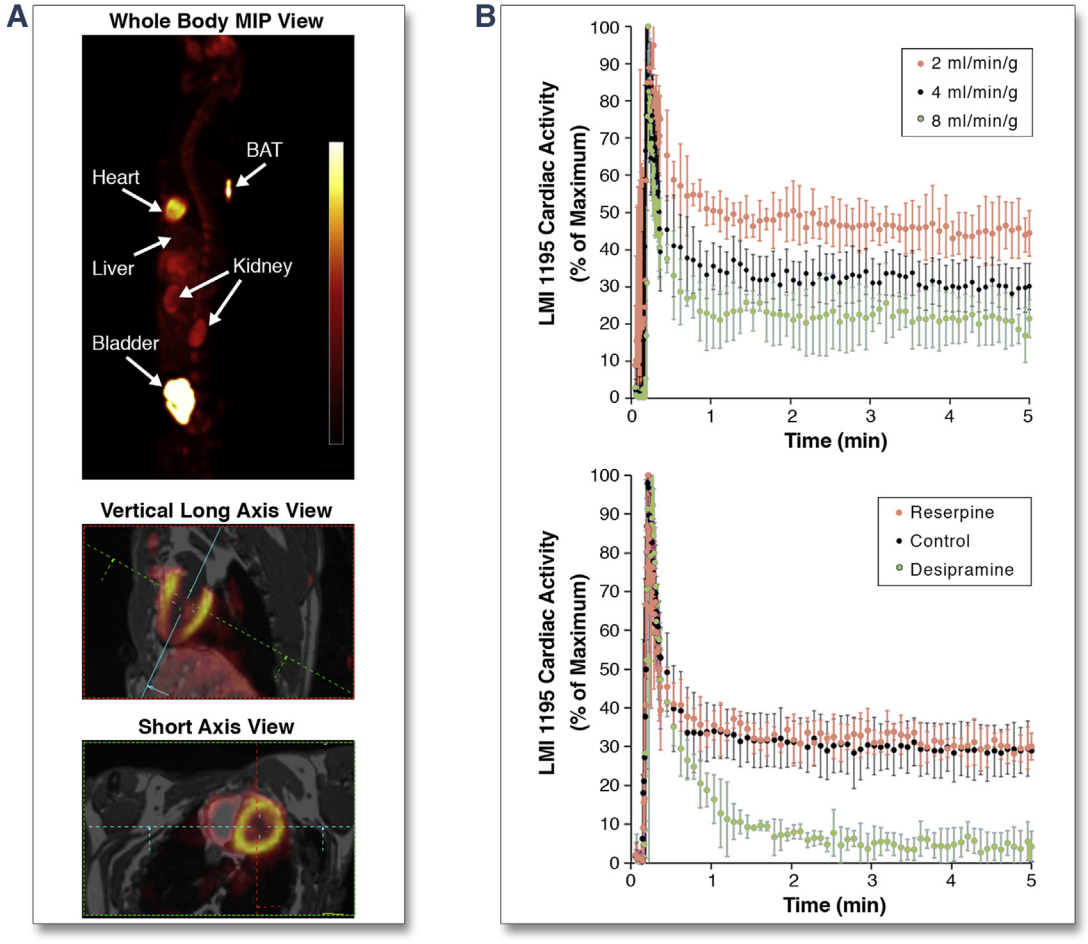

(A) In vivo [^{18}F]-LMI1195 positron emission tomography images of a rabbit using a clinical positron emission tomography–cardiac magnetic resonance system. High-contrast left ventricular delineation is seen, with minimal tracer activity in the surrounding tissues. **(B)** Averaged extraction time activity curves from [^{18}F]-LMI1195 cardiac uptake and washout studies in several isolated rabbit hearts. Flow-dependent decrease of tracer extraction is observed after bolus tracer administration **(top)**. Desipramine decreased the tracer extraction, whereas reserpine pre-treatment did not change the extraction **(bottom)**. BAT = brown adipose tissue; MIP = maximal intensity projection.

The mechanistic insights of [^{18}F]-LMI1195 uptake assessed in an isolated heart model might be relevant in the design of clinical imaging protocols, as well as the interpretation of imaging results in patients. However, further complementary in vivo animal experiments are needed to confirm and extended these findings for clinical studies.

Takahiro Higuchi, MD, PhD*
Behrooz H. Yousefi, PhD
Sybille Reder, MT
Monika Beschorner, MT
Iina Laitinen, PhD
Ming Yu, MD
Simon Robinson, PhD
Hans Jürgen Wester, PhD
Markus Schwaiger, MD
Stephan G. Nekolla, PhD

*Department of Nuclear Medicine
University of Würzburg
Oberdürrbacher Strasse 6
D-97080 Würzburg
Germany
E-mail: higuchi_t@klinik.uni-wuerzburg.de

http://dx.doi.org/10.1016/j.jcmg.2014.11.013

Please note: Drs. Yu and Robinson are employees of Lantheus Medical Imaging. All other authors have reported that they have no relationships relevant to the contents of this paper to disclose. Drs. Higuchi and Yousefi contributed equally to this work.

REFERENCES

1. Yu M, Bozek J, Lamoy M, et al. Evaluation of LMI1195, a novel ^{18}F-labeled cardiac neuronal PET imaging agent, in cells and animal models. Circ Cardiovasc Imaging 2011;4:435–43.

2. Higuchi T, Yousefi BH, Kaiser F, et al. Assessment of the ^{18}F-labeled PET tracer LMI1195 for imaging norepinephrine handling in rat hearts. J Nucl Med 2013;54:1142–6.

3. Sinusas AJ, Lazewatsky J, Brunetti J, et al. Biodistribution and radiation dosimetry of LMI1195: first-in-human study of a novel ^{18}F-labeled tracer for imaging myocardial innervation. J Nucl Med 2014;55:1445–51.

Novel Use of Cardiac Magnetic Resonance Imaging for the Diagnosis of Cobalt Cardiomyopathy

A 54-year-old male patient with bilateral metal-on-metal hip prosthesis and recently diagnosed cobalt toxicity presented with gradually worsening symptoms of heart failure. Serum cobalt (120 μg/l; normal <1 μg/l) and chromium (108.8 μg/l; normal <1.4 μg/l) levels were significantly elevated. Echocardiogram showed biventricular dysfunction (Online Video 1), and coronary angiogram was normal. Contrast-enhanced cardiac magnetic resonance (CMR) was performed for further evaluation of the non-ischemic cardiomyopathy.

CMR showed severe biatrial enlargement with reduced left ventricular ejection fraction (36%) and right ventricular ejection fraction (39%) (Online Video 2). Black-blood T2 images showed diffuse increased signal intensity (**Figures 1A and 1B**) and imaging after late gadolinium enhancement (LGE) revealed diffuse hyperenhancement of the left ventricle (**Figures 1C and 1D**).

Endomyocardial biopsy was performed (**Figures 1E and 1F**). Iron, Congo red, and thioflavin T stains for amyloid were negative. The patient underwent replacement of both hip prostheses, which were found to be surrounded in brown creamy fluid indicative of metallic debris. After surgery, cobalt (16.6 μg/l) and chromium (32 μg/l) levels declined. Repeat CMR was performed 5 months later and did not show any improvement in biventricular function, T2 imaging, or LGE. The patient continued to decline clinically and needed left ventricular assist device implantation.

The degree of hyperenhancement seen indicated a systemic etiology for the cardiomyopathy. This pattern of hyperenhancement is typically seen with cardiac amyloidosis; however, the blood pool kinetics were not consistent with amyloidosis. The toxic levels of cobalt and chromium and the absence of an alternative cause make cobalt cardiomyopathy the most likely diagnosis. The diffuse enhancement on LGE represented the diffuse fibrosis as seen on the endomyocardial biopsy in the patient and also seen in other reported cases (1,2). To our knowledge, this is the first report of using CMR in a patient with suspected cobalt cardiomyopathy. Because there are no confirmatory tests for this diagnosis (2), our findings suggest that CMR may have a role in establishing the diagnosis of cobalt cardiomyopathy. Moreover, in most previously described case reports (2,3), surgical removal of the metal-on-metal hip prosthesis resulted in clinical improvement. However, in our patient, despite a decrease in serum cobalt and chromium concentrations post-surgery, there was continued clinical deterioration. It is possible that the CMR findings as seen in our patient may be indicative of a poor prognosis in patients with cobalt cardiomyopathy.

Huma Y. Samar, MD*
Mark Doyle, PhD
Ronald B. Williams, BA
June A. Yamrozik, BS
Mark Bunker, MD
Robert W.W. Biederman, MD
Moneal B. Shah, MD